

A Design of Wireless Communication and Wireless Energy Transfer System for In-Pipe Robots

Jonathan Akafua, Ryan Chapman, and Hongzhi Guo
Engineering Department

Norfolk State University, Norfolk, VA, USA, 23504

Email: j.akafua@spartans.nsu.edu; r.d.chapman@spartans.nsu.edu; hguo@nsu.edu

Abstract—In-pipe robots and underground sensors play an important role in pipeline inspection by providing accurate sensing data. Some of the pipes are made of metal and buried underground. Radio Frequency (RF) signals in such an extreme environment experience significant propagation loss and uncertainty. This paper designs a hybrid wireless energy transfer and wireless communication system for in-pipe robots and underground sensors. The acoustic signals are used for wireless energy transfer. Low Frequency (LF) and High Frequency (HF) magnetic fields are used for through-pipe and near-pipe communications. Full-wave simulations are performed to evaluate the performance. A software-defined communication testbed is designed using QPSK modulation for LF and HF communications. The data rate and wireless channel are measured and analyzed. The results show that at the end of an 8 mm thick metal pipe, the maximum data rate is 50 kbps with a distance of 2 cm and 100 kHz carrier frequency.

Index Terms—Acoustic, extreme environments, internet of things, magnetic induction, near field communication, pipeline monitoring.

I. INTRODUCTION

Underground pipeline monitoring is a challenging problem due to the isolated underground extreme environment, where typical terrestrial wireless communication technologies do not work. Wireless underground sensors are deployed close to the pipe to externally monitor the status, while in-pipe robots are used to internally inspect the thickness of the pipe, sense the pressure of liquid/gas, and collect various other information to predict and detect leakages. Even today, data communication for underground sensors and in-pipe robots relies on wired technologies, e.g., the intelligent pigs used to internally inspect metallic pipes are tethered with a cable. Although Zigbee [1] and LoRa [2], [3] have been adopted for underground wireless communication, when it comes to wireless communication inside or close to a metal pipe, these technologies experience severe attenuation losses.

The acoustic waves and magnetic fields are two widely used mechanisms for through-metal wireless communication and wireless energy transfer [4], [5]. The review in [6] shows that both acoustic waves and magnetic fields have demonstrated sufficient efficiency, but it is not clear what is the optimal conditions to use them. In this paper, we propose a hybrid wireless communication and wireless energy transfer system

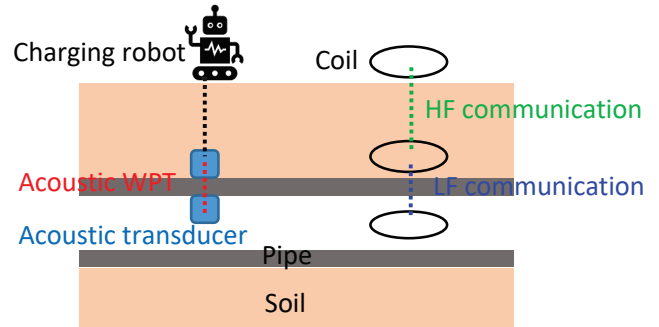


Fig. 1: Illustration of the proposed system. Wireless energy transfer uses acoustic waves where the piezoelectric transducers are attached to the pipe surface and the transmitter is connected to a charging robot. Through-pipe communication uses LF communication and the through-soil communication uses HF communication.

for in-pipe robots and underground sensors. The system leverages the advantages of acoustic waves and magnetic fields.

As shown in Fig. 1, the system consists of three different channels. First, acoustic waves are used for wireless energy transfer thanks to their high efficiency. The transducers are attached to the pipe surface. The external transmitter is connected to a charging robot and the internal receiver is installed on an in-pipe robot. Second, the through-pipe communication uses LF (Low Frequency Band) magnetic communication. The pipe is made of various materials, e.g., plastic, steel, and aluminum, depending on the utilities. LF signals have a long wavelength, which can penetrate through inhomogeneous media efficiently. However, LF signals rely on large coils due to the weak coupling. Third, the through-soil communication uses HF (High Frequency Band) signals which have stronger coupling with smaller coils compared to LF signals. The coil in the soil can be designed with dual bands using variable capacitors that can operate at both LF and HF bands.

This paper aims to understand the advantages and applicable conditions for the acoustic waves and LF and HF magnetic signals in order to leverage them for wireless communication and wireless energy transfer. To study the efficiency of acoustic wireless power transfer, we perform full-wave simulations in COMSOL Multiphysics using various frequencies with

different in-pipe materials. Then, we use full-wave simulations to visualize the magnetic field distribution for through-metal LF and HF magnetic fields using the configuration in our experiments. Lastly, we design a software-defined LF and HF communication testbed using USRP and coils. A metal pipe is used to build an in-lab testbed. The received power and bit-error-rate (BER) are measured.

The rest of this paper is organized as follows. The related works, including state-of-the-art acoustic and magnetic communication mechanisms and performances, are presented in Section II. The full-wave simulations of acoustic signals and magnetic fields are presented in Section III. A software-defined communication system using QPSK modulation is designed and tested in Section IV. Finally, this paper is concluded in Section V.

II. RELATED WORK

Various research works have been done to transmit both data and power through the pipe wall, especially metallic pipes. The first method of through-metal communication that has been quite extensively researched is the acoustic signal. The works in [7], [8], [9] and [10] propose designs that implement the coaxially aligned piezoelectric transducers at each side of a metal wall to transmit data across it using acoustic signals. Nevertheless, the efficiency of communication is highly dependent on the coupling material and the accuracy in coupling. Moreover, a slight shift in the position of the coupling transducers can result in a drastic reduction in communication efficiency. Recently, the use of Multiple-Input and Multiple-Output (MIMO) systems has shown significant advantages to reduce multipath fading and misalignment losses [4].

The second approach uses magnetic induction or resonance with low frequency to penetrate through dense media, such as metal walls and soil [5], [11]. The low-frequency magnetic field is decoupled from electric field in the deep near field, which can efficiently penetrate through high-permittivity and high-conductivity materials. In [12], a system architecture is proposed that makes use of pressure and acoustic sensors at the hub layer and soil property sensors at the in-soil sensor layers. These sensors can communicate with each other through a magnetic induction waveguide with coils on the pipeline. However, the deployment and operation cost of this technique for leakage detection is high and is yet to be deployed on a large-scale underground testbed. These are further posed as major challenges according to [12].

Besides acoustic waves and magnetic resonance/induction, capacitive coupling is also used [6]. There are also implemented systems for underground pipeline monitoring such as in [13] that employ Bluetooth and the Internet for communication in a wireless sensor network. [14] compared full-duplex/half-duplex systems with Sequential RFID tags placed outside the walls of the magnetic carbon steel pipe. It achieves a long communication range of more than 1 m. However, this system design does not refer to its performance on non-

magnetic pipes and has its mode of communication outside the pipe.

III. ACOUSTIC WAVE AND MAGNETIC FIELD SIMULATIONS

A. Acoustic Signals

Through-metal wireless communication and power transfer using acoustic signals demonstrate high data rates and high efficiency, respectively [4], [15]. However, acoustic signals rely on direct contact with the metal wall to obtain a high efficiency. For acoustic signals, if the pressure is $p_{acous}(d)$, then the intensity is

$$i_{acous}(d) = p_{acous}^2(d)/Z(d) \quad (1)$$

where $Z(d)$ is the specific acoustic impedance. The received power can be expressed as

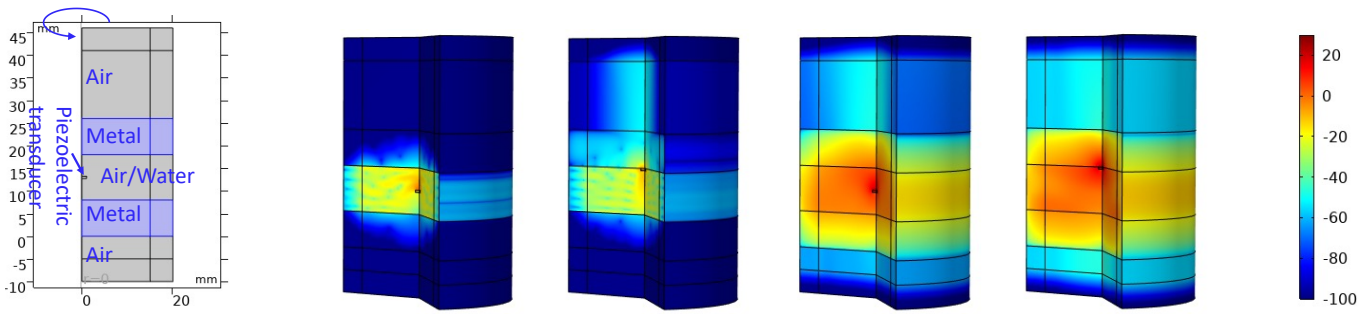
$$P_{acous}(d) = i_{acous}(d)A \quad (2)$$

where A is the area of the receiver [16]. We implicitly assume the receiving piezoelectric is perfectly aligned and there is no loss caused by direction. To visualize acoustic wave propagation through metal walls, we conduct full-wave simulations in COMSOL Multiphysics.

The propagation of the acoustic wave is affected by the material and the associated sound speed. Since the sound speed varies significantly in metal, liquids, and gases, there are strong reflections at the media boundaries. In the simulation, we numerically evaluate the received power. The simulation model is shown in Fig. 2a. COMSOL Multiphysics Acoustic Module with the axis-symmetric model is used. A piezoelectric transducer is placed in the middle of two metal plates. The thickness of the metal plate is 8 mm. The distance between the two plates is 10 mm. The piezoelectric transducer is 1 mm in radius and its thickness is 0.5 mm. The perfectly matched layer is used to avoid reflections from boundaries. To simulate the materials that are contained inside the metal-constrained environment, we consider the air (gas) and water (liquid). The piezoelectric is placed in the middle of the two metal plates and attached to the upper metal plate. The input voltage of the piezoelectric is 100 V. The sound intensity at 100 kHz in dB scale is shown in Fig. 2b.

As shown in Fig. 2b, the sound intensity in water is higher than that in the air. The sound velocity in the air (344m/s) is much smaller than that in metal (3100 m/s in Aluminum). While the sound velocity in water is (1480 m/s), which is much larger than that in the air. Therefore, the reflection loss from the boundary is small in water. Also, the sound intensity is higher when penetrating through the metal plate if the piezoelectric is attached to it. As presented in existing works [4], [15], the piezoelectric transducers are attached tightly to the metal surface to achieve a high efficiency. Otherwise, due to strong reflections, the efficiency can be reduced dramatically.

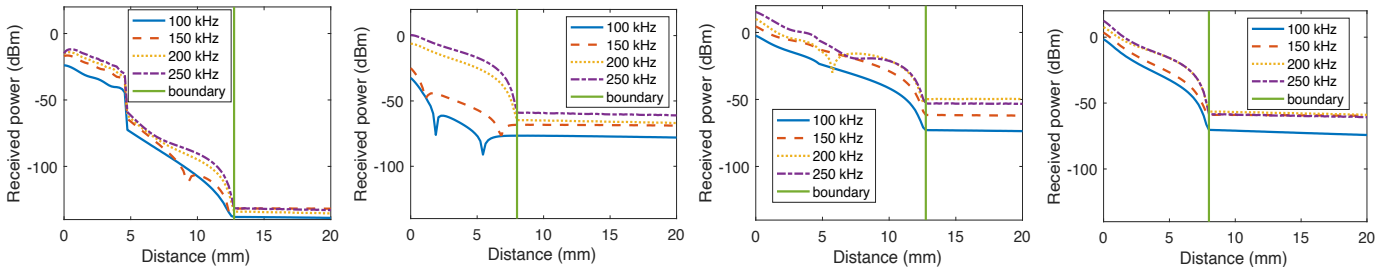
In Fig. 3, we plot the received power by using a virtual piezoelectric receiver of the same size as the transmitter. The



(a) Illustration of the geometry of axis-symmetric simulation model.

(b) From left to right: piezoelectric transducer (1) in the middle of the air, (2) in the air and attached to the upper metal layer, (3) in the middle of water, and (4) in water and attached to the upper metal layer. The intensity of sound is displayed in dB scale.

Fig. 2: Acoustic intensity (in dB) simulation at 100 kHz. The simulation model is 2D axis-symmetrical, i.e., the defined geometrical model will be rotated for 360° with respect to the axis. The piezoelectric transducer is placed in the middle of two metal plates or attached to the top metal plate. The thickness of the metal plates is 8 mm and the distance between two metal plates is 10 mm.



(a) Medium: air; the piezoelectric is in the middle

(b) Medium: air; the piezoelectric is attached to the top metal plate.

(c) Medium: water; the piezoelectric is in the middle

(d) Medium: water; the piezoelectric is attached to the top metal plate.

Fig. 3: Received power of piezoelectric. It is assumed that the receiver can be placed in any medium, including the metal.

receiver is placed along the axis from the top surface of the piezoelectric transducer and extends for 20 mm. The metal-air boundary at $z=26$ mm in Fig. 2a is also shown. We implicitly consider the receiver can be placed anywhere, including in the metal plate. For the scenario where the piezoelectric is attached to the metal plate, the metal-air boundary is closer to the top surface of the piezoelectric. Consistent with the illustration in Fig. 2b, when the piezoelectric is in water, the received power is much higher than that in the air. Also, the received power is lower than -140 dBm when the piezoelectric is in the air and not attached to the metal plate. We also simulated 150 kHz, 200 kHz, and 250 kHz. The performance is similar. The results indicate that for liquid, the location of piezoelectric does not affect the received power significantly because the reflection loss from the water-metal boundary is small. On the contrary, the location of piezoelectric plays an important role in the air. As shown in Fig. 3a and Fig. 3b, when the piezoelectric is in the middle of the two metal plates, the received power reduces by more than 100 dB. This is mainly due to the reflection loss from the air-metal surface.

In general, the simulation results suggest that if both the

transmit piezoelectric and the receive piezoelectric are attached to the two sides of a metal wall, the power loss can be as low as 50 dB for an 8 mm thick aluminum wall. However, if they are not attached to the aluminum wall, the received power becomes extremely small. Thus, the use of acoustic signals relies on direct contact with the metal wall. Also, perfect alignment is another key to obtain high efficiency. Static sensors can easily meet these requirements, but mobile robots cannot due to their mobility and larger operation areas.

In the proposed system, wireless energy transfer uses piezoelectric. Because a high volume of energy will be transmitted and we require a high efficiency. Compared to large LF coils, the piezoelectric is small, which is easy to be installed on a robot. Also, results show that the use of lower MHz band is even more efficient [4]. The piezoelectric requires alignment, which is not trivial since the transmitter and the receiver cannot see each other. This can be addressed by using magnetic fields to align their direction and location.

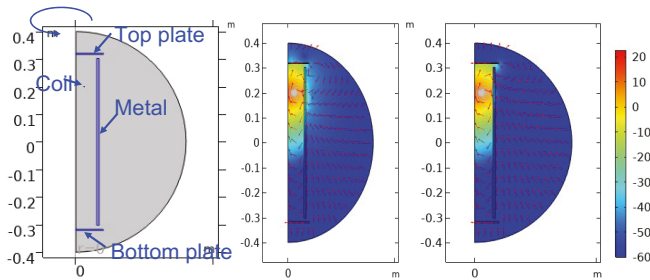


Fig. 4: Magnetic field (A/m) generated by a single turn coil with 1 A current (displayed in dB scale). Figures from left to right: (a) geometry of the simulation model, a small gap between the top and bottom plates and the metal wall is left intentionally to simulation our experiment setup in Section V; (b) magnetic field at 100 kHz; (c) magnetic field at 13.56 MHz.

B. Simulation of LF and HF Magnetic Field Propagation

Low-frequency magnetic fields in the deep near field can efficiently penetrate through most of the materials, including metal. An analytical model is provided in [5]. In the following, we provide a full-wave simulation to show the penetration efficiency with different frequencies.

As shown in Fig. 4, the axis-symmetric model in AC/DC module in COMSOL Multiphysics is used. The thickness of the aluminum wall is 8 mm. At the top and bottom, two aluminum plates with a thickness of 3 mm are used to close the pipe. In our experiment in Section IV, we notice that the plates cannot close the pipe tightly. Therefore, in the simulation model, we intentionally leave a gap between the plates and the metal pipe. The coil is placed close to an end of the pipe to simulate the experiment set up. As shown in Fig. 4, the 100 kHz magnetic field can slightly penetrate through the metal wall, but the 13.56 MHz is completely blocked. Some magnetic fields are leaking from the gap. Also, we notice that the magnetic fields do not require direct contact with the metal wall, which provides more flexibility for mobile robots. Although the coil also needs to be aligned, this can be addressed by using tri-axis coils [17]. The 13.56 MHz magnetic communication is used for NFC (near field communication). The peer-to-peer mode can be used for through-soil communication [11]. Since the soil has much lower conductivity than metal, the HF band signals experience less attenuation and the higher frequency provides stronger coupling.

IV. LF AND HF COMMUNICATION SYSTEM DESIGN

A. System Design

The magnetic communication system consists of the hardware part and the software part. The hardware uses coils and the USRP N210. The 100 kHz coil is designed using an AWG 20 wire which is wound with 120 turns to give an inductance of 1.72 mH and 2.71 mH to form the transmitter and receiver coils, respectively. These coils are hand-made and they have

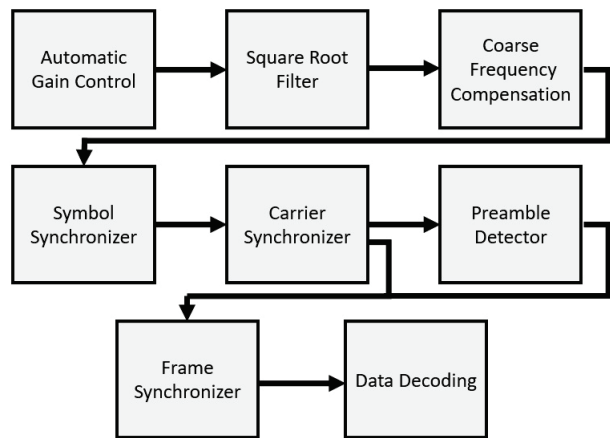


Fig. 5: Block diagram of communication using USRP.

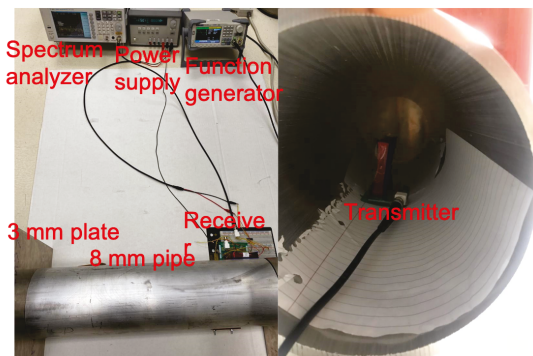


Fig. 6: Experiment setup. The two ends of the metal pipe is blocked by two metal plates.

different inductances. Resonance capacitors were connected in parallel to the coils to yield an operating frequency of about 100 kHz. The receiver circuit also uses an impedance matching circuit and an amplifier with 30 dB gain to increase the power of signals. The 13.56 MHz HF communication uses a commercialized coil ANT1356M from Eccel Technology.

The software is implemented in MATLAB with the USRP support from the Communications Toolbox. The Simulink model is adapted from the QPSK example [18]. We vary the symbol rate to control the transmission data rate. Also, the carrier frequency is changed to 100 kHz for the LF communication and 13.56 MHz for the HF communication. A block diagram of the receiver is shown in Fig. 5. The Square Root Filter is used for pulse-shaping to limit inter-symbol interference. The Coarse Frequency Compensation is responsible for compensating for the offset. The Symbol Synchronizer uses the Gardner algorithm. The Preamble Detector searches for Barker's code and the Frame Synchronizer gets the data ready for decoding.

B. Experiments and Discussions

To assess the performance of LF through-metal communication, the 100kHz transmitter is connected to the function generator and placed about 28 cm (in reference to the pipe's

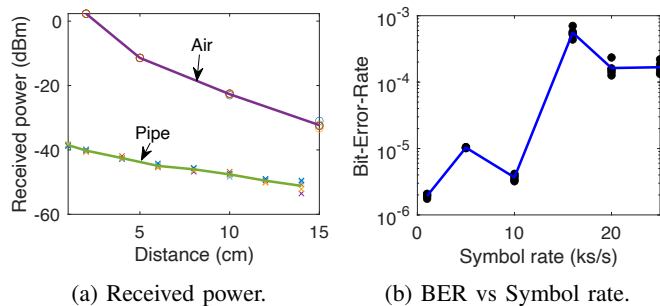


Fig. 7: Received power and BER for the 100 kHz coil inside of the pipe.

length) inside an aluminum pipe of thickness 8 mm and length 62 cm, as shown in Fig. 6. The receiver is placed at a varied distance between 16 cm to 30 cm from the edge of the pipe's length and its distance from the pipe's cross section was varied. The function generator generates a sinusoidal voltage of 5 V peak-to-peak. We observe that as the distance of the receiver from the pipe's cross section is increased, the received power decreases. The received power is insignificant after a distance 30 cm from the pipe's cross section since the noise floor is about -50 dBm. A comparison between the received power when the coil is in the pipe (close to one end of the pipe's length) and when the coil is outside of the pipe (in the air) is shown in Fig. 7a. It shows that the received power reduces significantly when the coil is in the pipe. We also notice that if we put the coil in the middle of the pipe, the received power further reduces and the BER increases significantly. This is because the metal may completely block the signal. In our experiment, we place the coil close to one end of the pipe, signals may leak from the gap as shown in Fig. 4. A similar setup is used for the 13.56 MHz NFC commercialized coil. When the transmitter is placed in the pipe, the received power at the center frequency is at the noise floor of about -47 dBm. This indicates that even there is a small portion leakage of the magnetic field from the pipe end, the 13.56 MHz is strongly affected by the metal environment and it cannot send any signal out. This motivates us to use even lower frequencies, such as the VLF band, in our future work.

A similar experiment was carried out with a transmitter outside the pipe but close to the pipe. This is used for the through-soil communication where one of the coils is placed close to the pipe. The experiment was conducted in the air. Due to the long wavelength, the impact of the soil is weak. The received power was measured with the receiver at varying distances. The received power of both the 100 kHz coil and the NFC coil was reduced as compared to when the transceivers are not close to any metal.

Next, we use the software-defined radio testbed to measure the BER. The USRP is connected via a local area network (LAN) and the transmitter block is connected to the transmitter coil. We place the transmitter coil in the metallic pipe; the same as the previous setup. The USRP receiver has a different

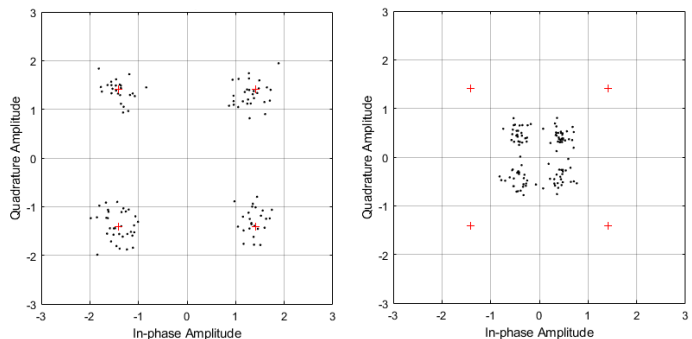


Fig. 8: Constellation at the after carrier synchronizer stage of the 100 kHz set up when transmitter in pipe. The USRP gain, symbol rate, center frequency and roll-factor are set to 71 dB, 1000 s/s, 100 kHz and 0.5, respectively. From left to right: (a) constellation when the receiver is 1 cm away from the pipe; (b) constellation when the receiver is 2 cm away from the pipe.

IP address from the transmitter. It is connected to the receiver circuit. The center frequency, symbol rate, gain, and roll-off factor are set to 100 kHz, 1000 Symbol/s, 71 dB, and 0.5, respectively.

The USRP setup is used to measure the BER at varied symbol rates with the transmitter coil placed in the pipe. Both coils are however placed close to the ends of the pipe with the receiver distance fixed at 2 cm away from the pipe. It was realized that the BER at 32 kbps increased sharply but reduced beyond 32 kbps. Nevertheless, there is still a general increase in BER with increasing symbol rate, as shown in Fig. 7b. The maximum data rate we obtain is 50 kbps with a BER lower than 0.001. To achieve reliable communication, the data rate should be lower than 20 kbps (10 ks/s) To measure the BER at different distances, the USRP testbed is used with the transmitter coil inside the pipe while the distance of the receiver from the pipe is varied. When the transmitter is placed inside the pipe around the midpoint, there is no observed signal and the BER is around 0.5. However, there is a received signal when the transmitter and receiver are about 2.5cm away from the end of the pipe as shown in the constellation in Fig. 8. As the distance increases by 1 cm, the received symbols start to get close. It shows that the signal power reduces very fast. This could be explained by the fact that the resonance frequency of the 100 kHz transceiver coils is not exactly 100 kHz. We also put the 13.56 MHz NFC coil in the pipe to transmit signals and the other coil outside of the pipe to receive signals. However, no matter how close the BER is around 0.5, which shows that the HF band cannot be used for through-pipe communication.

We also place the transmitter close to the pipe and measured the BER in the air. In the proposed system, there are sensors deployed outside of the pipe to relay data from in-pipe sensors/robots to receivers above ground. We use a 13.56 MHz coil and the received power is slightly above the noise floor and the BER is 0.0015 at 30 cm away with a 2 kbps data rate.

C. Future Work

Based on the results we obtained in this paper, our future work will focus on the following three aspects. First, according to the theoretical model in [5], the optimal frequency of magnetic fields to penetrate through the metal pipe will be around 1 kHz to 10 kHz. In this paper, we use 100 kHz and we can only receive signals when the transmitter is placed close to the pipe ends. We will design VLF coils and try to minimize their size. The software need also to be updated to adapt to such low frequency transmission. After that, we will perform experiments to verify its performance. Second, we will study the impact of the metal environment on coil impedance, which causes a mismatch of impedance. The coil misalignment will also be considered. Third, we will use the empirical study to evaluate the wireless energy transfer efficiency using piezoelectric.

V. CONCLUSION

Autonomously monitoring the underground pipeline is a challenging task due to the lack of wireless communication support. This paper proposes a design of wireless communication and wireless energy transfer system for underground wireless sensors and in-pipe robots. Acoustic waves are used for wireless energy transfer and LF (low frequency) and HF (high frequency) signals are used for wireless communications. Full-wave simulations are performed to study the wireless energy transfer and wireless communication performance. A software-defined testbed is developed using USRP and hand-made coils. The performance of the proposed communication system is tested under various configurations. Future research needs to be done in reducing the signals from LF to VLF, i.e., around 1 kHz to 10 kHz, to increase the efficacy of through metal communication.

ACKNOWLEDGMENT

The authors would like to thank D. W. Pitts and C. M. Witts for their assistance and insightful comments.

REFERENCES

- [1] M. A. Moridi, Y. Kawamura, M. Sharifzadeh, E. K. Chanda, and H. Jang, "An investigation of underground monitoring and communication system based on radio waves attenuation using zigbee," *Tunnelling and Underground Space Technology*, vol. 43, pp. 362–369, 2014.
- [2] D. W. Sambo, A. Forster, B. O. Yenke, I. Sarr, B. Gueye, and P. Dayang, "Wireless underground sensor networks path loss model for precision agriculture (wusn-plm)," *IEEE Sensors Journal*, vol. 20, no. 10, pp. 5298–5313, 2020.
- [3] K. Lin and T. Hao, "Experimental link quality analysis for lora-based wireless underground sensor networks," *IEEE Internet of Things Journal*, vol. 8, no. 8, pp. 6565–6577, 2020.
- [4] J. D. Ashdown, L. Liu, G. J. Saulnier, and K. R. Wilt, "High-rate ultrasonic through-wall communications using mimo-ofdm," *IEEE Transactions on Communications*, vol. 66, no. 8, pp. 3381–3393, 2018.
- [5] H. Guo and K. D. Song, "Reliable through-metal wireless communication using magnetic induction," *IEEE Access*, vol. 7, pp. 115 428–115 439, 2019.
- [6] D.-X. Yang, Z. Hu, H. Zhao, H.-F. Hu, Y.-Z. Sun, and B.-J. Hou, "Through-metal-wall power delivery and data transmission for enclosed sensors: A review," *Sensors*, vol. 15, no. 12, pp. 31 581–31 605, 2015.
- [7] R. P. Welle, "Ultrasonic data communication system," Nov. 9 1999, uS Patent 5,982,297.
- [8] G. J. Saulnier, H. A. Scarton, A. J. Gavens, D. Shoudy, T. Murphy, M. Wetzel, S. Bard, S. Roa-Prada, and P. Das, "P1g-4 through-wall communication of low-rate digital data using ultrasound," in *2006 IEEE Ultrasonics Symposium*. IEEE, 2006, pp. 1385–1389.
- [9] R. Primerano, K. Wanuga, J. Dorn, M. Kam, and K. Dandekar, "Echo-cancellation for ultrasonic data transmission through a metal channel," in *2007 41st Annual Conference on Information Sciences and Systems*. IEEE, 2007, pp. 841–845.
- [10] R. Primerano, M. Kam, and K. Dandekar, "High bit rate ultrasonic communication through metal channels," in *2009 43rd Annual Conference on Information Sciences and Systems*. IEEE, 2009, pp. 902–906.
- [11] H. Guo and A. A. Ofori, "The internet of things in extreme environments using low-power long-range near field communication," *IEEE Internet of Things Magazine*, vol. 4, no. 1, pp. 34–38, 2021.
- [12] Z. Sun, P. Wang, M. C. Vuran, M. A. Al-Rodhaan, A. M. Al-Dhelaan, and I. F. Akyildiz, "Mise-pipe: Magnetic induction-based wireless sensor networks for underground pipeline monitoring," *Ad Hoc Networks*, vol. 9, no. 3, pp. 218–227, 2011.
- [13] I. Stoianov, L. Nachman, S. Madden, and T. Tokmouline, "Pipeneta wireless sensor network for pipeline monitoring," in *Proceedings of the 6th international conference on Information processing in sensor networks*, 2007, pp. 264–273.
- [14] B. Tye and R. Vyas, "A test comparison of full/half duplex and sequential rfid systems for communication with magnetic carbon steel pipes," in *2019 IEEE 62nd International Midwest Symposium on Circuits and Systems (MWSCAS)*. IEEE, 2019, pp. 540–543.
- [15] V. F.-G. Tseng, S. S. Bedair, and N. Lazarus, "Acoustic power transfer and communication with a wireless sensor embedded within metal," *IEEE Sensors Journal*, vol. 18, no. 13, pp. 5550–5558, 2018.
- [16] M. Yuan, Z. Cao, J. Luo, and X. Chou, "Recent developments of acoustic energy harvesting: A review," *Micromachines*, vol. 10, no. 1, p. 48, 2019.
- [17] H. Guo, Z. Sun, and P. Wang, "Joint design of communication, wireless energy transfer, and control for swarm autonomous underwater vehicles," *IEEE Transactions on Vehicular Technology*, vol. 70, no. 2, pp. 1821–1835, 2021.
- [18] MathWorks. (Accessed in Jul. 2021) QPSK Transmitter with USRP Hardware. [Online]. Available: <https://www.mathworks.com/help/supp ortpkg/usrpradio/ug/qpsk-transmitter-with-usrp-r-hardware.html>